

Evaluation of wireless sensor networks (WSNs) for remote wetland monitoring: design and initial results

Carl J. Watras · Michael Morrow · Ken Morrison · Sean Scannell · Steve Yaziciaglu · Jordan S. Read · Yu-Hen Hu · Paul C. Hanson · Tim Kratz

Received: 27 March 2013 / Accepted: 6 September 2013 / Published online: 18 September 2013
© Springer Science+Business Media Dordrecht 2013

Abstract Here, we describe and evaluate two low-power wireless sensor networks (WSNs) designed to remotely monitor wetland hydrochemical dynamics over time scales ranging from minutes to decades. Each WSN (one student-built and one commercial) has multiple nodes to monitor water level, precipitation, evapotranspiration, temperature, and major solutes at user-defined time intervals. Both WSNs can be configured to report data in near real time via the internet. Based on deployments in two isolated wetlands, we report highly resolved water budgets, transient reversals of flow path,

rates of transpiration from peatlands and the dynamics of chromophoric-dissolved organic matter and bulk ionic solutes (specific conductivity)—all on daily or sub-daily time scales. Initial results indicate that direct precipitation and evapotranspiration dominate the hydrologic budget of both study wetlands, despite their relatively flat geomorphology and proximity to elevated uplands. Rates of transpiration from peatland sites were typically greater than evaporation from open waters but were more challenging to integrate spatially. Due to the high specific yield of peat, the hydrologic gradient between peatland and open water varied with precipitation events and intervening periods of dry out. The resultant flow path reversals implied that the flux of solutes across the riparian boundary varied over daily time scales. We conclude that WSNs can be deployed in remote wetland-dominated ecosystems at relatively low cost to assess the hydrochemical impacts of weather, climate, and other perturbations.

C. J. Watras · K. Morrison
Wisconsin Department of Natural Resources, UW-Trout Lake Research Station,
Boulder Junction, WI 54512, USA

C. J. Watras (✉) · K. Morrison · P. C. Hanson · T. Kratz
Center for Limnology, University of Wisconsin-Madison,
180 North Park St., Madison, WI 53706, USA
e-mail: cjwatras@wisc.edu

M. Morrow · S. Scannell · S. Yaziciaglu · Y.-H. Hu
Department of Electrical and Computer Engineering,
University of Wisconsin-Madison,
Madison, WI, USA

J. S. Read
Department of Civil and Environmental Engineering,
University of Wisconsin-Madison,
Madison, WI, USA

Present Address:
J. S. Read
Center for Integrated Data Analytics, U.S. Geological Survey,
Middleton, WI 53562, USA

Keywords Wireless sensor networks · Ecosystem observatories · Wetlands · Dissolved organic carbon · Climate change

Introduction

Since the pioneering work of Mainwaring et al. (2002) and Szweczyk et al. (2004), wireless sensor networks (WSNs) built on low-power microprocessor-radio hardware platforms (MPRs) have become ever more promising tools for environmental monitoring (Chong and Kumar 2003;

Baronti et al. 2007; Kido et al. 2008; Porter et al. 2009; Ritsema et al. 2009; Barnhart et al. 2010). Environmental WSNs typically consist of an array of sensor nodes that are embedded in the environment to collect data at user-defined time intervals. The nodes are designed to run unattended on battery power for time periods of weeks to years, often using just a few 1.5-V batteries as the power source. Nodes can be configured as self-healing meshes, stars, or daisy-chains; but regardless of topology, they ultimately communicate through a gateway to a distant base station via radiofrequency (RF) signals. Field data can then be broadly disseminated over the Internet, often in near-real time, thus forming a science network of investigators and resource managers.

The purpose of this paper is to describe and evaluate the potential of low-power WSN technology to monitor the hydrochemistry of wetlands as weather and climate evolve in the future. Wetlands are prominent features of the landscape in many regions of the world and they provide essential ecosystem services such as flood abatement, water quality improvement, aquifer recharge, and biodiversity enhancement as well as climate modulation through carbon sequestration and latent heat transfer (Johnson et al. 2005; Mitra et al. 2005; Mackay et al. 2007; Limpens et al. 2008; Heinemeyer et al. 2010). At our location in the heavily forested Northern Highland Lake District (NHLD) of northern Wisconsin and upper Michigan, wetlands cover ~20 % of the district's 7,000 km² surface area (Buffam et al. 2010). They provide critical habitat for endemic flora and fauna, and they store an estimated 144±21 Tg of carbon in deep peatlands—an amount that is 130 % larger than the mass of carbon stored in the upland soils and forest biomass combined (63±3 Tg C; Buffam et al. 2011). Thus, climatic shifts that alter the water balance of these wetlands could simultaneously reduce biodiversity and mobilize a vast carbon reservoir, potentially exacerbating the greenhouse warming effect (Bridgman et al. 2006).

This work focuses on two prototype WSNs: one built in-house by undergraduate students and one obtained commercially as a turn-key system. Both WSNs monitor wetland water levels and key elements of wetland water budgets (precipitation, evapotranspiration, and water storage), along with the bulk concentration of ionic solutes (specific conductance) and chromophoric-dissolved organic carbon (the major constituent of peatland pore waters and bog ponds). The two networks have been deployed since 2009, and they function in tandem with the Global Lakes Ecological Observatory Network at the

University of Wisconsin's Trout Lake Research Station (www.gleon.org). Here, we describe the technology and deployment protocols, and we evaluate WSN reliability, data quality, and utility.

Methods and materials

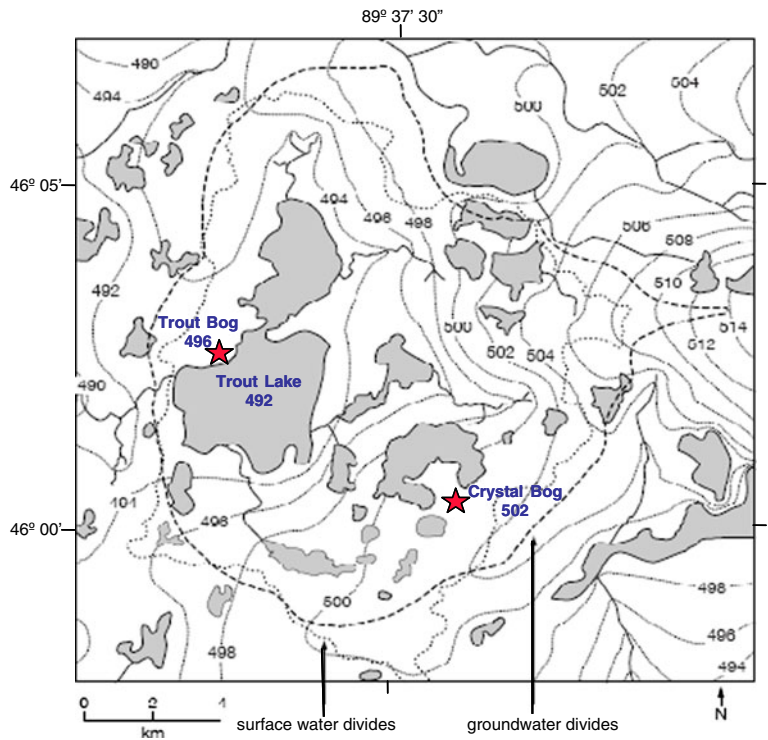
Study sites

WSNs were deployed in two small wetlands within the Trout Lake watershed, a catchment nested within the NHLD (Fig. 1). Wetlands constitute roughly 7 % of the 130 km² watershed, along with 115 lakes and ponds which have a combined surface area of 30 km² (Magnuson et al. 2006). Groundwater elevations vary from about 492–514 m asl with Trout Lake being the terminal discharge point. The Crystal Bog subcatchment is situated at a relatively high elevation in the watershed, and it comprises a sparsely forested peatland (7 ha) surrounding a shallow bog pond (0.5 ha; 2.5 m deep) that has no channelized inflow or outflow. The Trout Bog subcatchment is more heavily forested and situated lower in the landscape (Kratz et al. 2006). It comprises a peatland (4.5 ha) surrounding a deeper bog pond (1.1 ha, 7.9 m deep) that also has no tributary or distributary streams. Maximum peat thickness in both wetlands is ~10 m. Additional details on the study sites are available at www.lter.limnology.wisc.edu and www.wetlands.gleon.org.

IT Infrastructure in Crystal Bog

The Crystal Bog WSN was built in-house on the MICA2 and MDA300 hardware platforms (<http://www.memsic.com>). The nodes have five main components: (1) the MICA2 MPR, (2) the MDA300 DAQ board, (3) the main board PCB, (4) battery packs, and (5) the sensors (Fig. 2a–c). As shown in Fig. 2c, the first four components are housed in a waterproof enclosure. The MICA2s run data acquisition firmware and transmit sensor data via 903 MHz RF to the gateway. They form a self-healing and multihopping mesh network, which means they establish their own lines of communication that self-adjust to interference and optimize network topology. The network requires four software tiers (Fig. 3): (1) XMesh™ (Memsic) resides on the MICA2s to run networking algorithms required for reliable communication among all the nodes within the mesh cloud; (2) CRBasic™ (Campbell

Fig. 1 Trout Lake watershed showing the location of the two wetlands under study (after Webster et al. 2006)



Scientific) resides on the datalogger to store serial data and add time stamps; (3) LoggerNet™ (Campbell Scientific)

resides on the base station computer to poll the datalogger at user-defined time intervals; and (4) miscellaneous

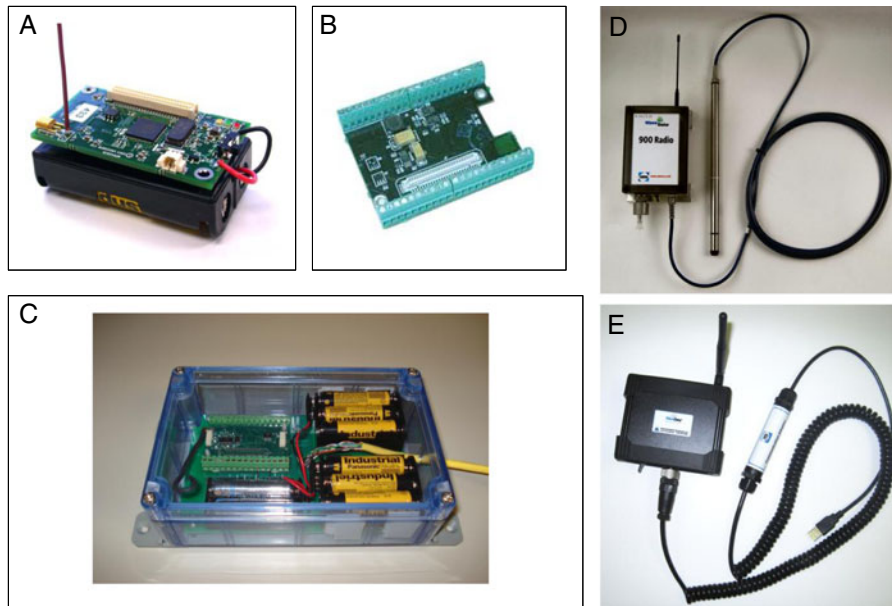
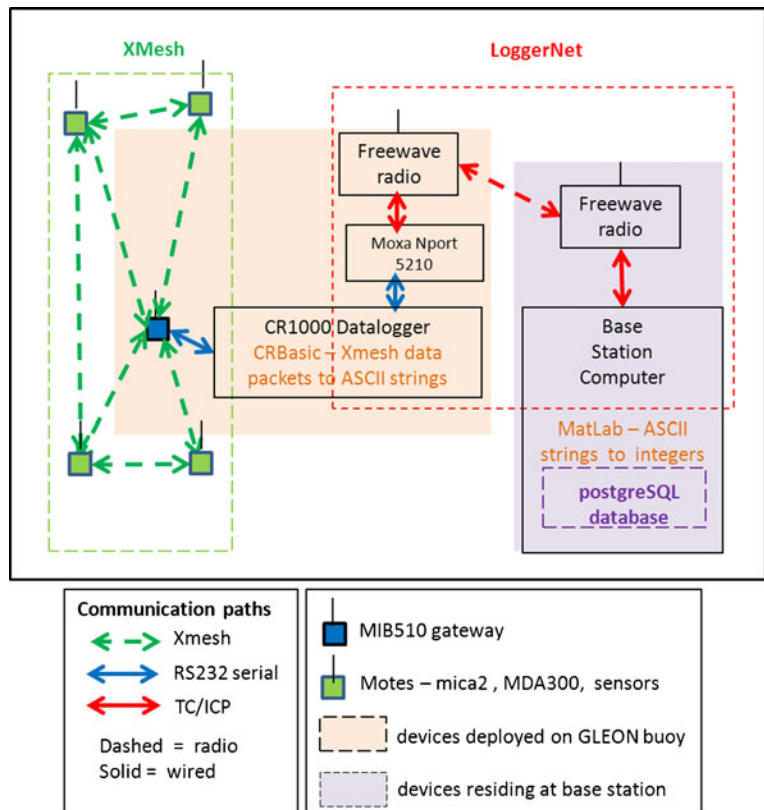


Fig. 2 Radiosensor components. **a–c** Components assembled by undergraduate students for deployment in Crystal Bog. **a** MICA2 microprocessor MPR; **b** MDA320 data acquisition board (DAQ); **c** field enclosure housing the MPR, DAQ board, printed circuit board (PCB), batteries, and cable to sensors. **d, e**

Pre-assembled units obtained commercially (photos complements of INW, Inc.) for deployment in Trout Bog; **d** MPR in field enclosure attached to datalogging CTD sensor, **e** portable gateway transceiver with USB connector

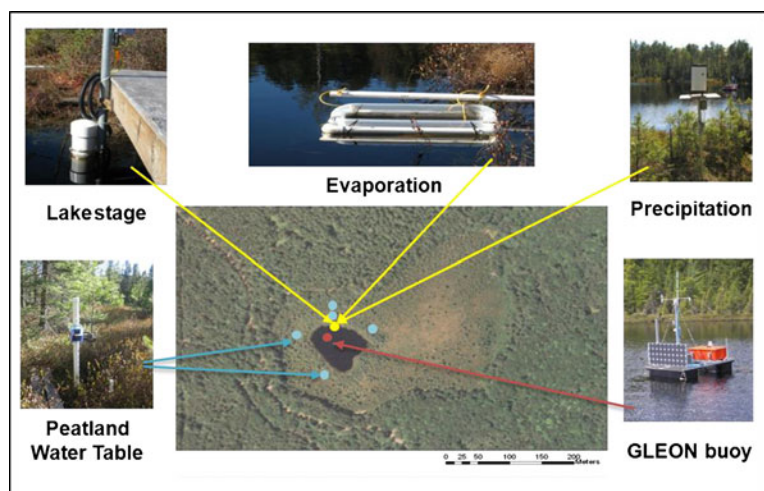
Fig. 3 IT infrastructure in the Crystal Bog WSN (see text “IT Infrastructure in Crystal Bog” section)



software packages, such as Excel™ and MatLab™, provide data analysis services at the base station. The sensors are powered by 12 AA 1.5 V batteries and the MICA2 is powered by 2 C cell 1.5-V batteries. With these power sources, network lifetime was estimated conservatively to be 4–6 weeks based on our criterion of changing batteries when voltages approached 2.7 V.

The physical layout of the Crystal Bog WSN is shown in Fig. 4. The network comprises nodes that monitor water level, temperature, specific conductance, precipitation, evaporation, and chromophoric dissolved organic matter (CDOM) at user-defined time intervals (usually 15–30 min in our application). There are three sensors at most nodes: a WL400 barometrically compensated water

Fig. 4 Physical layout of the Crystal Bog WSN. *Blue dots* peatland wells; *red dot* GLEON buoy; *yellow dot* colocation of stilling well (lake stage), evaporation pan, and rain gauge (see “IT Infrastructure in Crystal Bog” section for details)



level sensor, a WQ301 specific conductivity sensor (both from Global Water Instrumentation, Inc.; <http://www.globalw.com/>) and a temperature probe (U.S. Sensor p/n USP7881; <http://www.ussensor.com/>). A serial transceiver base station (Memsic MIB510), a Campbell Scientific datalogger (CR1000), a Moxa™ serial device driver (Nport 5210), and a 1 W FreeWave™ spread spectrum radio (FGR-115RE) comprise the hub of the WSN and reside on a GLEON buoy moored on the pond. The MIB510 base station aggregates data from the mesh network and interfaces with the datalogger through a RS232 serial bus. The packets are framed using a PPP_HDLX protocol. The CR1000 converts the XMesh packets to ASCII strings and forwards them through a serial RS232 connection with the Nport 5210 device server which integrates these serial messages into a private TC/ICP network for transmission via the Freewave radios to the base station. A computer at the research station running LoggerNet™ polls the datalogger at hourly time intervals to acquire the serial data, where Matlab™ scripts parse strings into integers and inserts them into a PostgreSQL database.

As indicated in Fig. 4, there are five nodes in the peatland which consist of water table wells made from 2" ID Schedule 40 PVC pipe with horizontal slots (0.01") extending from 0.5 to 1.25 m below the peat surface (well screen #WS2001; <http://www.aquaticceco.com>). The sensors in each well measure water level, temperature, and specific conductance (as a proxy for bulk ionic solute concentrations). The pond node consists of a stilling well (6" ID PVC pipe) that houses a water level sensor. The sensors outside the stilling well measure specific conductance, temperature, and CDOM in the pond water. Rainfall is monitored with a tipping bucket rain gauge and each tip is relayed to the gateway by a small MICA2/MDA300 unit that runs on 2 AA batteries. Evaporation is monitored with an in situ evaporation pan that consists of a clear plastic box that floats in the bog pond. The E-pan is 40 cm wide×35 cm deep×50 cm long. It is filled with pond water and outfitted with a flotation collar so that the top is elevated a few cm above the surface of the pond. A water level sensor and thermistor are mounted on the bottom of the E-pan. It is manually tended once per week to compensate for rainfall input and evaporative loss.

The elevation of nodes that monitor water level were all referenced to a common geographic benchmark and resurveyed at least once each year. To further constrain the effect of peat elasticity on the elevation of wells over

time, long rods were driven into the peat beside each well to the point of refusal (7–12 m below the peat surface). The elevational difference between the top of the rod and the top of the adjacent monitoring well was measured periodically to track vertical displacement of wells. As shown in Fig. 5, the elevation of wells varied by about ±2 cm over a 3.5 year time period, and the seasonal pattern of movement was relatively uniform across the peatland.

IT Infrastructure in Trout Bog

The WSN in Trout Bog consists of commercial WaveData™ radiosensor units obtained from Instrumentation Northwest (INW), Inc. of Kirkland, WA, USA (Fig. 2d). Each node has a submersible, data-logging sensor connected to a 10 mW radio transceiver. The sensor units can log 520,000 data records internally with programmable, multiphase sequence capabilities. They record and output data over either Modbus® or SDI-12 communication protocols. Radio communication and data processing are facilitated by Aqua4Plus™, a Windows-based GUI from INW with dropdown menus to program and calibrate sensors, download files, and display data in graphical or tabular formats. The sensors are powered by two AA batteries, which act as a backup power source when connected to the 8 AA batteries that power the radio transceiver.

The physical layout of the Trout Bog WSN is shown in Fig. 6. Node installation was similar to that in Crystal Bog except that the peatland nodes were arranged in three

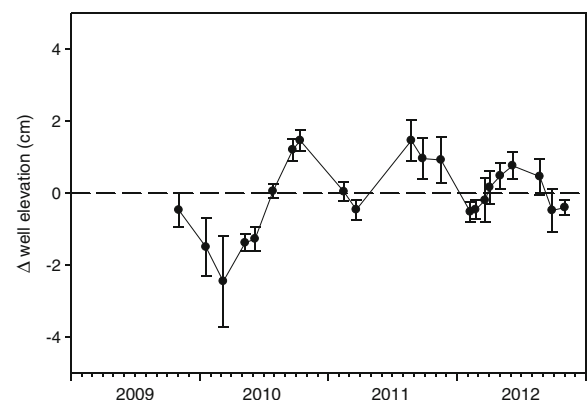
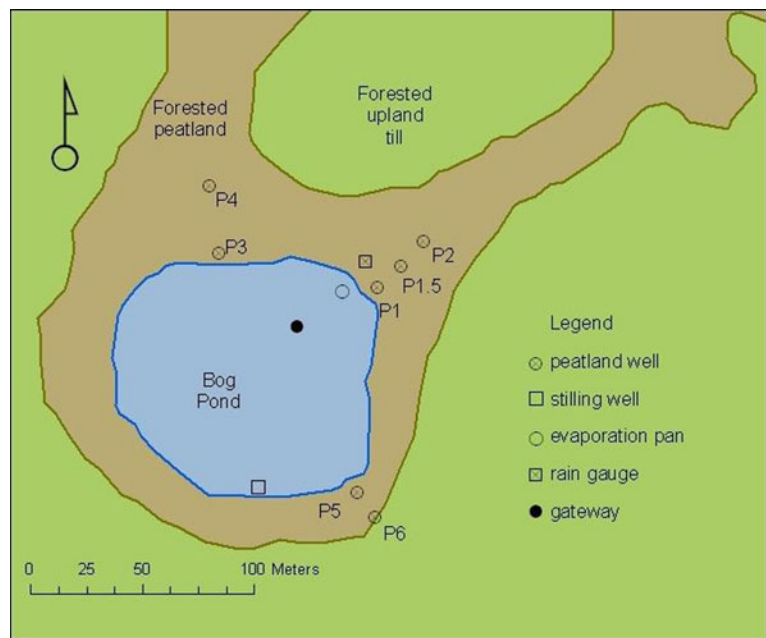


Fig. 5 Seasonal changes in the elevation of monitoring wells in the Crystal Bog peatland attributable to peat elasticity. Data are the deviation from the long-term mean elevation for each of five wells, shown as the average deviation and range for each date

Fig. 6 Location of WSN nodes in the Trout Bog wetland. Peatland wells were arranged to form three transects running perpendicular to the pond



transects extending away from the pond. The INW radios do not form a mesh network. Instead, they each communicate directly to the gateway on the GLEON buoy in the pond. As in Crystal Bog, the gateway is hardwired to a Freewave™ ethernet radio (FGR-115RE) that communicates with a computer at the Trout Lake Station. Nodes can be accessed using a virtual private network from any remote location with Internet connectivity. Nodes can also be accessed onsite using a mobile communication package that consists of a netbook connected to a 10-mW radio transceiver via a USB/RS-485 adapter (Fig. 2e). Local line-of-sight communication has a range of about 200 m in the heavily forested Trout Bog catchment. This communication range is sufficient to access all nodes from one location in the surrounding upland without disturbing the wetland.

Estimating water budgets and evapotranspiration rates

Since there are no surface inflows or outflows from either wetland complex, water budgets for the two bog ponds were based on the water balance equation: $\Delta S = P - E + G_{\text{net}}$, where ΔS represents the change in storage (water level), P is direct precipitation, E is evaporation, and G_{net} is the net subsurface exchange between the pond and the peatland. The variables ΔS and P were measured directly, E was determined from the E -pan and G_{net} was estimated by difference. As a preliminary validation of the E -pan methodology, we compared E -pan rates to estimates of E based

on a Bowen ratio–energy balance (BREB) model (Lenters et al. 2005). For the Trout Bog pond during a 10-day period of dry weather in August 2010, estimates of E (mean±SD) were 3.4 ± 0.89 mm/day for the E -pan and 3.0 ± 0.65 mm/day for the BREB model (no statistically significant difference at $\alpha=0.95$, paired t test).

Budgets for peatland waters conformed to a similar water balance equation, substituting evapotranspiration (ET) for E . The modified White method for deconstructing diurnal water table fluctuations was used to estimate ET rates (White 1932). The method permits subdaily estimates of ET by decomposing daily fluctuations into two processes: (1) a drawdown during daylight hours due to consumption by vegetation and (2) a continuous refill due to subsurface inflow. ET rates were calculated using Eq. (1) from Loheide (2008):

$$ET_G(t) = S_Y^* \left[\Gamma(WT_{DT}(t)) + m_T - \frac{dWT}{dt} \right] \quad (1)$$

where $ET_G(t)$ is the rate of water loss from the saturated zone due to transpiration (in millimeter per time), S_Y^* is the readily available specific yield of the peat (dimensionless), dWT/dt is the rate of change in water table depth (in millimeter per time), and the remaining terms constitute the net inflow (recovery) rate (in millimeter per time). S_Y^* was estimated using the precipitation infiltration method wherein the relationship between ΔWT and precipitation amount was established as an empirical function of water table depth (Gerla 1992; Rosenberry and Winter 1997).

The net inflow (recovery) rate is estimated as the sum of the linear trend in water table, m_T , and the best fit estimate, $\Gamma(\text{WT}_{\text{DT}})$ of the functional relation between the recovery rate and the water table level in the detrended data (Loheide 2008).

Monitoring CDOM

CDOM sensors were deployed from the GLEON buoys in the center of each bog pond. The sensors are in situ optical devices that measure CDOM fluorescence as a proxy for dissolved organic carbon concentration. Two commercial CDOM sensors were deployed: (1) the C3 Submersible Fluorometer from Turner Designs, Inc (Sunnyvale, CA, USA) and (2) the SeaPoint UV Fluorometer from SeaPoint Sensors, Inc. (Exeter, NH, USA). Since the SeaPoint sensor did not have a biofoul wiper, it was configured with a flowcap and a SeaBird™ 5 M submersible pump. The pump was activated 1 min prior to energizing the sensor and deactivated thereafter. The sensors were calibrated in Trout Bog water prior to deployment to ensure comparability of readings. All CDOM data were referenced to a standard temperature (20 °C) and reported as CDOM₂₀ (Watras et al. 2011).

Results and discussion

Water budgets for the Bog Ponds

Daily integrated water budgets for Crystal Bog during 2010 illustrate how precipitation events and evaporation affect water level fluctuations and flow paths between the ponds and the peatlands (Fig. 7). Water levels in the pond initially declined during an exceptionally dry spring and then rebounded with rainfall that began in June. The pond hydrograph shows recurrent episodes of rapid rise followed by gradual drawdown in response to individual rain events. Evaporation from the pond followed a relatively smooth sigmoidal trend with accelerated rates during midsummer. Seepage was highly variable over very short time scales. This behavior can be seen more clearly when the seepage term is plotted on an expanded scale (Fig. 8). During June, seepage was primarily toward the pond with daily rates approaching 25 mm. As summer progressed, seepage loss from the pond dominated while seepage into the pond occurring sporadically in response to individual rain events. Integrated over the entire open water season, there was a net seepage loss of about 50 mm which

constitutes a minor loss term compared to roughly 600 mm of evaporation. Although the absolute magnitude of subsurface influx and outflux cannot be inferred from net seepage rates alone, the daily budgets imply that peatland pore waters tended to pulse into the pond during rain events and then, during intervening periods of dry weather, there was gradual seepage loss from the pond into the peatland. As described below, these flow path reversals have implications for solute transport pathways.

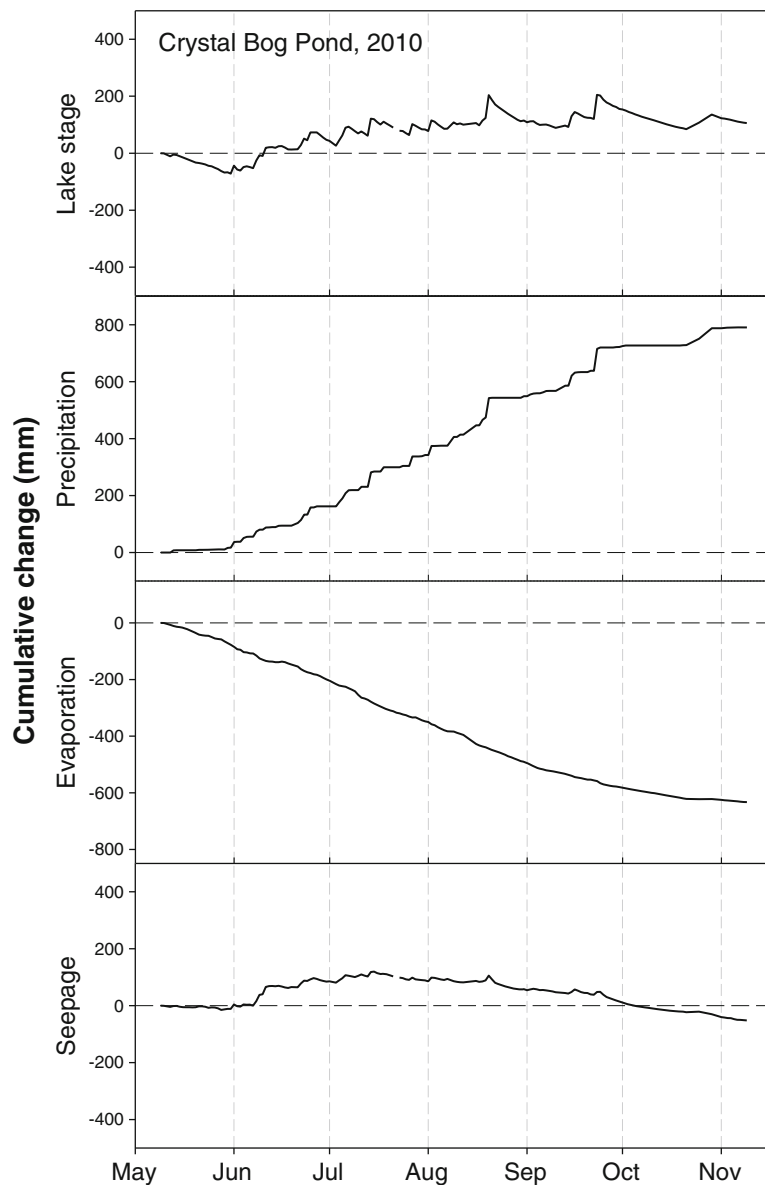
Monthly integrated water budgets are generally consistent with the conclusion that seepage rates were relatively low over the long term and that the net direction of subsurface flow between peatland and pond varied with time (Table 1). The monthly budgets are also consistent with the conclusion that evaporation was the dominant process governing water loss from the ponds. However, the frequency of flow reversals across the peatland/pond boundary and their relation to antecedent weather were not evident at a monthly time scale.

Daily water budgets for both bog ponds during 2012 indicate that the resolution of the two WSNs was comparable and that the hydrologic response to rain events was similar (with one notable anomaly) despite their different elevations in the Trout Lake watershed (Fig. 9). An interesting anomalous response was observed in Trout Bog during late October when the pond's water level rose abruptly by roughly 300 mm during a 60-mm rainfall event. Since no conspicuous sign of overland flow was evident and since the peatland water table rose by as much as 600 mm at some sites, the large water level gain implies rapid in-seepage from the peatland. Although the underlying cause remains unexplained, we note that the sandy upland bordering the peatland was subject to a commercial timber harvest shortly before the rain event. Since the entire event lasted only 48 h, it would not have been detected without high-frequency sampling.

Water table dynamics in the peatland

The hydrologic response to rainfall and dry out was greater in the peatlands due to displacement by peat solids (i.e., high specific yield). In Trout Bog, the largest response was generally at nodes furthest from the pond edge, presumably due to increases in the bulk density of peat with distance from open water. In the pond, the immediate response to rain ($\Delta\text{S:P}$) was typically 1:1; but in the peatland, the response ($\Delta\text{WT:P}$) was as high as 3:1 (Table 2). During a dry spring in 2010, hydrographs for the Trout Bog peatland show that the water table rose

Fig. 7 Daily water budgets for the Crystal Bog pond in 2010. Data are cumulative change from initial value set to zero (*dashed line*) on day 1 of time series



dramatically during snowmelt (~660 mm at site P2) and declined gradually thereafter, establishing a hydrologic gradient that extended away from the pond into the peatland (Fig. 10a,b). In response to a sequence of large rain events in July and August (Fig. 10c), transient water table mounds developed along peatland transect 1 (Fig. 10d). Mound duration was short (1–4 days per event), but the water table occasionally rose to a higher elevation than the bog pond. This observation is consistent

with conclusions about flow path reversals drawn from the daily water budgets.

The hydrographs for most peatland sites exhibited an abrupt water table rise at the onset of precipitation followed by a sharp decline soon after rainfall stopped as exemplified by Fig. 10b,d. This behavior implied that direct precipitation rather than groundwater discharge was the predominant source of water to the wetlands. If discharge from a deep groundwater system

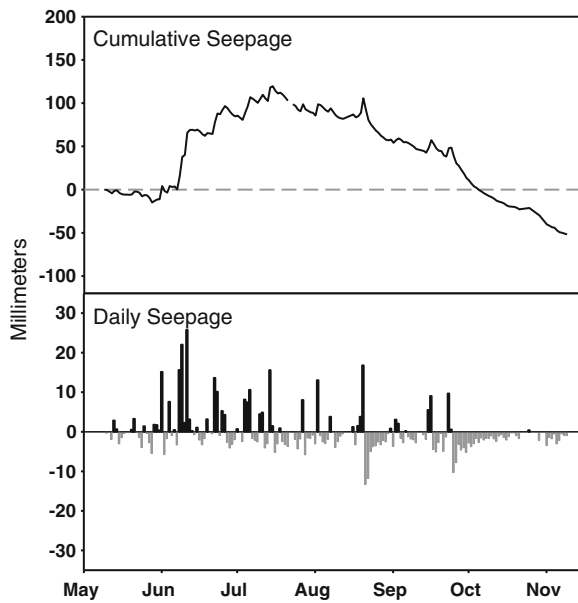


Fig. 8 Cumulative and daily seepage to and from the Crystal Bog pond during 2010

was an important source, one would expect the peatland hydrographs to show a time delay due to inflow after the cessation of rain (Hemond 1980). Even though both wetlands are adjacent to elevated uplands, and even though the peatlands are not obviously domed or sloped toward a conspicuous lagg or stream (cf. geophysical models of Ingram (1982) or Holden and Burt (2003)), the response to rainfall implies that they are perched above the local groundwater system. However, in the Trout Bog complex, one site provided an exception. At site P5, the hydrograph was often distinctly rounded after a precipitation event implying delayed inflow from a secondary source. Since the water table at

P5 typically remained below the elevation of the pond, we tentatively conclude that the delay was due to infiltration from the pond. Site P5 is adjacent to the 45m-wide sandy isthmus separating the Trout Bog pond from Trout Lake, which lies at an elevation ~1.8 m below the pond. The anomalous hydrograph implies that site P5 is within the wetland area where water is discharged toward Trout Lake.

The geophysical signature of transpiration is a conspicuous feature of most peatland hydrographs during the growing season (e.g., Fig. 10d). During drawdown after rainfall, the hydrographs show diurnal oscillations that first become evident during leaf-out in early May (e.g., Fig. 10b). Using Eq. (1), we calculated transpiration rates that varied from 2.2 to 9.1 mm/day across four peatland sites in the Trout Bog peatland during late August (Table 3). The grand mean for this time period was 4.8 mm/day, significantly higher than the corresponding evaporation rate from the pond (3.4 mm/day). The diurnal water table oscillations varied in shape depending on the site and the time period. This variability was simulated using a simple recursive model:

$$WT(t) = WT(t-1) + ET + G_{net} \tag{2}$$

where t represents the sensor sampling interval, ET is set to follow a sinusoidal diel photocycle and G_{net} represents the subsurface exchange with an area adjacent to the monitoring well. By varying the relative magnitudes of ET and subsurface flow, we could recreate the diurnal patterns observed in field data (Fig. 11).

Table 1 Monthly water budgets for Crystal Bog during 2010
Mean (mm/day)

Month	Days	Δ Storage	Precipitation	Evaporation	Seepage (net)
May	22	-3.2	0.8	-3.8	-0.2
June	30	4.0	4.8	-4.0	3.1
July	31	1.2	5.8	-4.7	0.1
August	31	1.0	6.7	-4.6	-1.0
September	30	1.4	5.8	-3.0	-1.5
October	31	-0.6	2.1	-1.3	-1.4
November	9	-3.3	0.3	-1.2	-2.5
Full Season	184	0.6	4.3	-3.4	-0.3

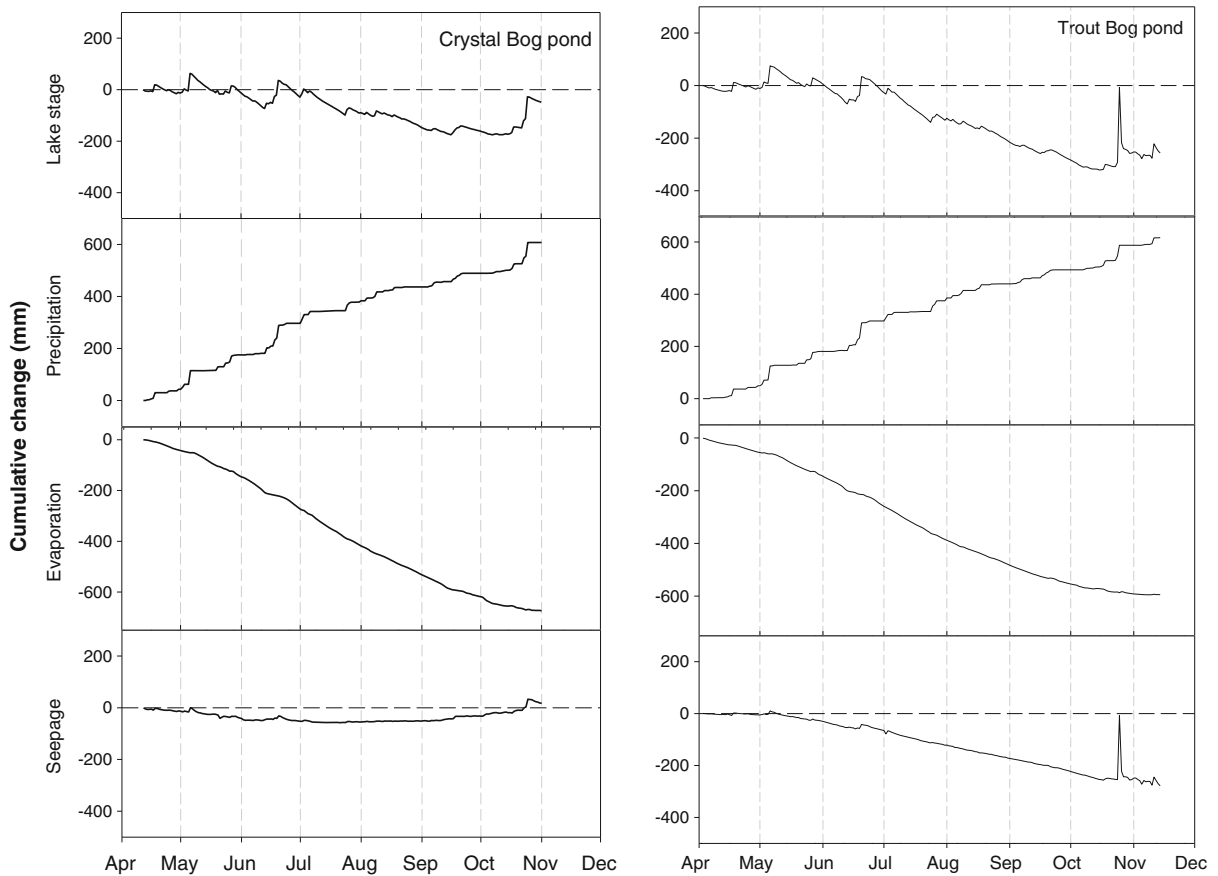


Fig. 9 Comparative water budgets for the Crystal Bog and Trout Bog ponds compiled daily for the ice-free season, 2012

Solute dynamics

Dissolved organic matter (DOM) is a major constituent of bog ponds and peatland porewaters, imparting their

Table 2 Rainfall infiltration and average specific yield at six peatland nodes in Trout Bog (based on linear regression of P vs Δ WT for 37 precipitation events between April and November 2010)

Peatland node	Δ WT:P	SE_x	CV(%)	S_Y^*
P1	1	0.08	7.9	1
P1.5	2.4	0.68	28.4	0.42
P2	3	0.53	17.3	0.33
P3	1.6	0.31	19.6	0.63
P4	2.8	0.44	15.8	0.36
P6	3	0.55	18.6	0.34

tea-stained appearance. In the Crystal Bog and Trout Bog ponds, DOM concentrations average roughly 8 and 18 mg C/L, respectively, while DOM in the peatland porewaters can exceed 60 mg C/L. The CDOM sensors were deployed to gain insight into the carbon flux across the riparian boundary between peatland and pond over short and long time scales. CDOM fluorescence was corrected for temperature quench using the method of Watras et al. (2011) which takes into account inner filtering by DOM over the range ~1 to 18 mg DOC/L. The conductivity sensors were deployed to compliment CDOM measurements because bulk ionic solutes would include H^+ and weak organic acid anions mobilized during peat decomposition as well as cations and anions from other sources.

The first time series for CDOM in Crystal Bog is shown in Fig. 12a. Although there are data gaps due to instrument retrieval for laboratory experimentation, the

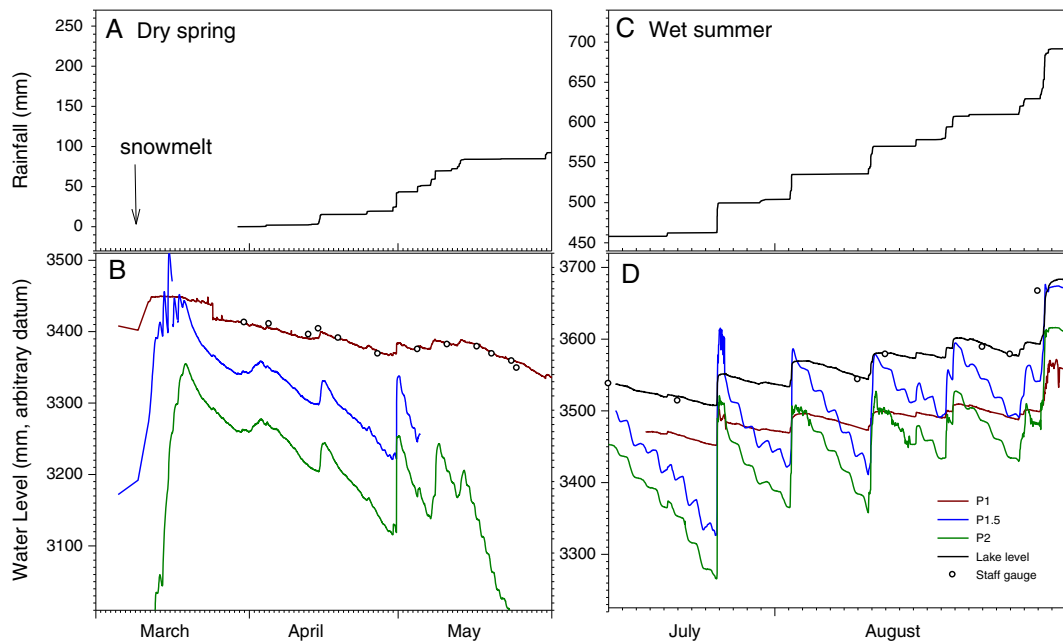


Fig. 10 Response of water levels in the Trout Bog pond and peatland to precipitation events and intervening periods of dry out during an exceptionally dry spring (a, b) and wet summer (c, d) in 2010

time series suggests that the concentration of DOM was relatively low in Crystal Bog during dry spring weather. After the rainy period began in mid-June, CDOM fluorescence increased by ~30 %, presumably due to increased export of DOM from the surrounding peatland. Mechanistically, CDOM would be expected to increase when in-seepage from the peatland exceeds the dilution effect of direct rainfall on the pond surface. The time series also shows that both CDOM sensors responded similarly even though their optical configuration was

quite different. Note that the two CDOM sensors were not cross calibrated for this first time series.

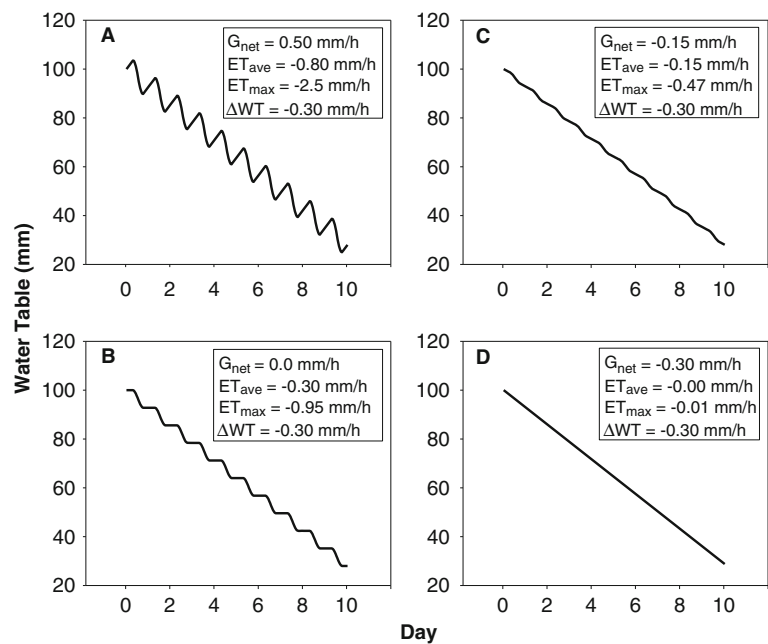
Time series for CDOM and specific conductivity in Trout Bog pond are compared in Fig. 12b. The two time series track each other reasonably well, an observation which suggests that pond water conductivity is largely attributable to the weak acid anions and H⁺ associated with DOM of peatland origin. This hypothesis is consistent with the observations of Marin et al. (1990) who reported strong direct correlations between specific con-

Table 3 Rates of evapotranspiration (ET_G) from nodes in the Trout Bog peatland during the time period from 21–31 August 2010. For comparison, the rate of evaporation (E) from the TB pond averaged 3.4 mm/day (range, ±1.3; SE_x, 0.1) during this time

Node	Evapotranspiration rate (mm/day)				Specific yield (S _Y [*])		
	Mean	Range	SE _x	n	Mean	Range	n ^a
P1.5	4.27	±1.79	0.15	9	0.60	±0.07	225
P2	3.45	±1.04	0.08	9	0.51	±0.04	225
P4	2.18	±0.45	0.03	9	0.56	±0.03	225
P6	9.12	±3.45	0.27	9	0.68	±0.03	225

^a A node-specific S_Y^{*} was calculated for each 30 min time interval between 6:00 am and 6:00 pm (25 points) over the full 9-day period

Fig. 11 Simulated hydrographs for the peatland water table that show the effect of varying the relative rates of transpiration loss (ET) and subsurface replenishment (G_{net}) when the rate of water table drawdown (ΔWT) is kept constant (based on Eq. (2)). All four patterns were observed in field data



ductivity, DOM, pH, and the anion deficit in porewaters of the Crystal Bog peatland.

Time series for conductivity and water level fluctuations are compared in Fig. 13. There was a gradual decline in the conductivity of pond water from May through August when the peatland water table at two of the three near-shore nodes was at or below the elevation of the pond (Fig. 13a). This downward trend was reversed during September when the peatland water table at all the near-shore nodes rose well above the level of the pond. The time series for CDOM exhibited a similar biphasic trend (data not shown). Two large spikes in pond water conductivity were associated with major rainfall events in July and August (Fig. 13b), but these spikes were not evident in the CDOM time series. This disparity may be due to the location of the two sensors. The conductivity sensor was located near-shore, in proximity to the presumed source of solutes. The CDOM sensor was located near the middle of the pond, where dilution of a riparian signal is potentially large. Thus, although the CDOM and conductivity sensors appear to track each other reasonable well over long time scales, they do not necessary track well over daily time-scales. To test this hypothesis in future deployments, we plan to colocate the two sensors near shore.

Conclusions and recommendations

The results from these initial deployments suggest that WSNs are a useful, relatively low-cost option for obtaining continuous, high-quality data on wetland hydrochemistry as weather and climate evolve over future years. The nodes deployed at Crystal Bog demonstrate that sensor networks can be constructed in-house if sufficiently skilled personnel are available. This is a reasonable expectation at many research universities and government laboratories. The in-house system described here went through several iterations as field experience was gained and as more sophisticated design and construction methods were employed by students. For those without access to the capability to build in-house, a network like that in Trout Bog can be assembled using off-the-shelf components. As one might expect, the decision to build in-house or use off-the-shelf components is a complex trade-off of time, cost and expertise.

With respect to technology needs, future wetland observatories would benefit from the automation and standardization of data handling and analysis protocols. Data management, processing, and dissemination pose a major challenge because the volume of data from embedded sensor networks can grow rapidly. In

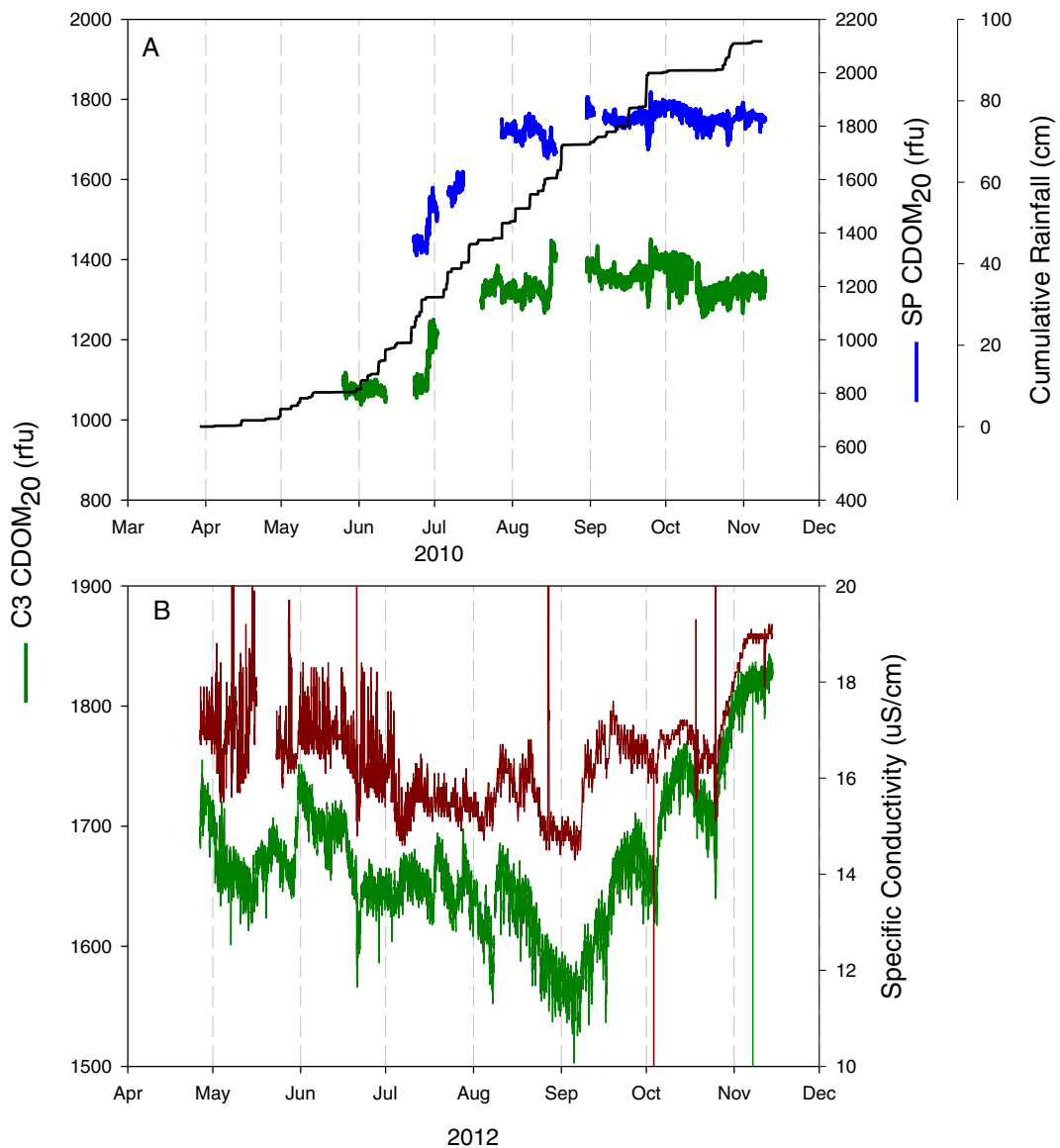


Fig. 12 Comparative time series for CDOM, rainfall and specific conductivity in the bog ponds. **a** Crystal Bog pond in 2010; C3 TurnerDesigns sensor, SP SeaPoint sensor. **b** Trout Bog pond

in 2012. $CDOM_{20}$ is the temperature-corrected value (Watras et al. 2011). *Rfu* relative fluorescence units

our small prototype networks, each node produces 35,000 to 45,000 data points per year. Thus, effective networks will require the allocation of substantial resources to technologies for data processing, quality assurance, database management, and dissemination.

With respect to wetland science, WSNs show considerable promise for providing insights into wetland

hydrology, geochemistry, and sensitivity to perturbation. For example, our preliminary data suggest that lateral flow reversals across the boundary between peatlands and surface waters can occur on daily time-scales in response to individual rainfall events and intervening periods of dry out. This finding may have profound significance with respect to current climate change

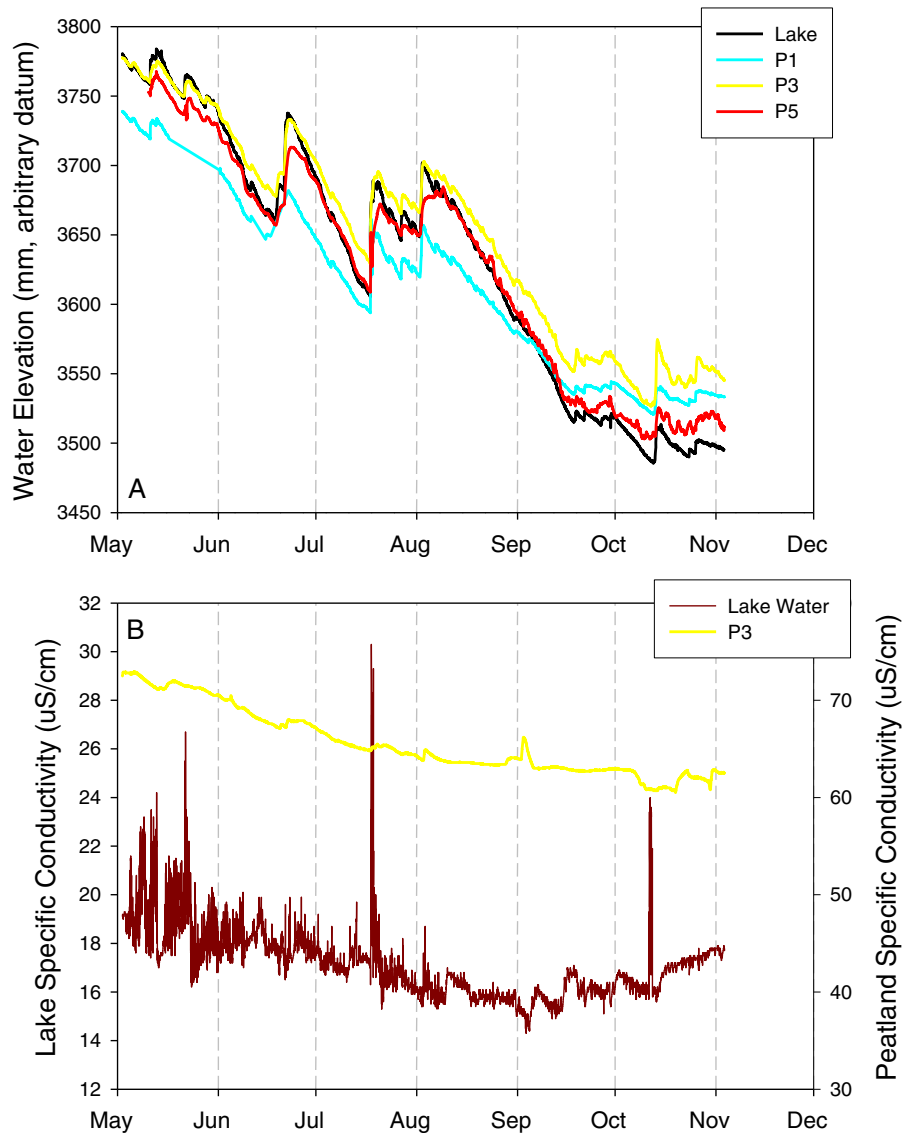


Fig. 13 Fluctuation of water levels and specific conductivity in Trout Bog during 2011. **a** Water level time series for the bog pond and three peatland wells located near shore. **b** Conductivity time series for the bog pond and a peatland well

scenarios and carbon mobilization. Flashier water tables and declining surface water levels are one potential consequence of a warmer and wetter climate. This scenario is considered likely for prairie pothole wetlands in the semi-arid Dakota region of North America (Rosenberry and Winter 1997), and it may also be likely for the now humid Great Lakes region as well. If the mobilization of peatland carbon depends on the frequency and magnitude of water level changes, then carbon fluxes between terrestrial, aquatic, and atmospheric pools could also be affected, feeding back positively on the warming effect

(Limpens et al. 2008; Heinemeyer et al. 2010). More broadly distributed wetland sensor networks would constitute a useful tool for tracking and modeling such climatic impacts over both short and long time scales (cf. Drexler and Ewel 2001).

Acknowledgments Funding was provided by the Wisconsin Focus on Energy-EERD Program (www.focusonenergy.com/Envi-ro-Econ-Research/) and the Wisconsin Department of Natural Resources. Logistical support was provided by the Global Lake Ecological Observatory Network (www.gleon.org) and by the North Temperate Lakes Long Term Ecological Research Project (www.

ter.limnology.wisc.edu/). We thank JR Rubsam for technical assistance in the field and laboratory, and we thank Harry Hemond for helpful discussions of wetland processes. The prototype nodes in Crystal Bog were built by Sean Scannell and Steve Yazicioglu, undergraduates in Electrical and Computer Engineering at UW-Madison, under the direct supervision of ECE instructor Mike Morrow. This is a contribution from the Trout Lake Research Station, University of Wisconsin-Madison.

References

Barnhart, K., Urteaga, I., Han, Q., Jayasumana, A., & Illangasekare, T. (2010). On integrating groundwater transport models with wireless sensor networks. *Ground Water*, *48*(5), 771–780. doi:10.1111/j.1745-6584.2010.00684.x.

Baronti, P., Pillai, P., Chook, V. W. C., Chessa, S., Gotta, A., & Hu, Y. F. (2007). Wireless sensor networks: a survey on the state of the art and the 802.15.4 and ZigBee standards. *Computer Communications*, *30*(7), 1655–1695. doi:10.1016/j.comcom.2006.12.020.

Bridgman, S. D., Megonigal, J. P., Keller, J. K., Bliss, N., & Trettin, C. (2006). The carbon balance of North American wetlands. *Wetlands*, *26*(4), 889–916.

Buffam, I., Carpenter, S. R., Yeck, W., Hanson, P. C., & Turner, M. G. (2010). Filling holes in regional carbon budgets: predicting peat depth in a north temperate lake district. *Journal of Geophysical Research*. doi:10.1029/2009JG001034.

Buffam, I., Turner, M. G., Desai, A. R., Hanson, P. C., Rusak, J. A., Lottig, N. R., et al. (2011). Integrating aquatic and terrestrial components to construct a complete carbon budget for a north temperate lake district. *Global Change Biology*, *17*, 193–1211.

Chong, C.-Y., & Kumar, S. P. (2003). Sensor network: evolution, opportunities and challenges. *Proceedings of the IEEE*, *91*(8), 1247–1256. doi:10.1109/JPROC.2003.814918.

Drexler, J. Z., & Ewel, K. C. (2001). Effect of the 1997–1998 ENSO-related drought on hydrology and salinity in a Micronesian wetland complex. *Estuaries*, *24*(3), 347–356.

Gerla, P. J. (1992). The relationship of water table changes to the capillary fringe, evapotranspiration, and precipitation in intermittent wetlands. *Wetlands*, *12*, 91–98.

Heinemeyer, A., Croft, S., Garnett, M. H., Gloor, E., Holden, J., Lomas, M. R., et al. (2010). The MILLENNIA peat cohort model: predicting past, present and future soil carbon budgets and fluxes under changing climates in peatlands. *Climate Research*, *45*, 207–226. doi:10.3354/cr00928.

Hemond, H. F. (1980). Biogeochemistry of Thoreau’s Bog, Concord, Massachusetts. *Ecological Monographs*, *50*(4), 507–526.

Holden, J., & Burt, T. P. (2003). Hydrological studies on Blanket Peat: the significance of the Acrotelm–Catotelm model. *Journal of Ecology*, *91*(1), 86–102.

Ingram, H. A. P. (1982). Size and shape in raised mire ecosystems: a geophysical model. *Nature*, *297*, 300–303.

Johnson, W. C., Millett, B. V., Gilmanov, T., Voldseth, R. A., Guntenspergen, G. R., & Naugle, D. E. (2005). Vulnerability of northern prairie wetlands to climate change. *Bioscience*, *55*(10), 863–872.

Kido, M. H., Mundt, C. W., Montgomery, K. N., Asquith, A., Goodale, D. W., & Kaneshiro, K. Y. (2008). Integration of wireless sensor networks into cyberinfrastructure for monitoring Hawaiian “Mountain-to-Sea” environments. *Environmental Management*, *42*(4), 658–666. doi:10.1007/s00267-008-9164-9.

Kratz, T. K., Webster, K. E., Riera, J. L., Lewis, D. B., & Pollard, A. I. (2006). Making sense of the landscape: geomorphic legacies and the landscape position of lakes. In J. J. Magnuson, T. K. Kratz, & B. J. Benson (Eds.), *Long-term dynamics of lakes in the landscape* (pp. 49–66). New York: Oxford.

Lenters, J. D., Kratz, T. K., & Bowser, C. J. (2005). Effects of climate variability on lake evaporation: results from a long-term energy budget of Sparkling Lake, northern Wisconsin (USA). *Journal of Hydrology*, *308*, 168–195.

Limpens, J., Berendse, F., Blodau, C., Canadell, J. G., Freeman, C., Holden, J., et al. (2008). Peatlands and the carbon cycle: from local processes to global implications—a synthesis. *Biogeosciences*, *5*, 1475–1491.

Loheide, S. P., II. (2008). A method for estimating subdaily evapotranspiration of shallow groundwater using diurnal water table fluctuations. *Ecohydrology*, *1*, 59–66.

Mackay, D. S., Ewers, B. E., Cook, B. D., & Davis, K. J. (2007). Environmental drivers of evapotranspiration in a shrub wetland and an upland forest in northern Wisconsin. *Water Resources Research*. doi:10.1029/2006WR005149.

Magnuson, J. J., Kratz, T. K., & Benson, B. J. (Eds.). (2006). *Long-term dynamics of lakes in the landscape (Long-term Ecological Research Network Series)*. Oxford: Oxford University Press.

Mainwaring, A., Polastre, J., Szewczyk, R., Culler, D., & Anderson, J. (2002). Wireless sensor networks for habitat monitoring. In: *Proceedings of the 1st ACM International Workshop on Wireless Sensor Networks and Applications (Atlanta, Sept.)*. New York: ACM Press. pp. 88–97.

Marin, L. E., Kratz, T. K., & Bowser, C. J. (1990). Spatial and temporal patterns in the hydrogeochemistry of a poor fen in northern Wisconsin. *Biogeochemistry*, *11*, 63–76.

Mitra, S., Wassmann, R., & Vlek, P. I. G. (2005). An appraisal of global wetland area and its organic carbon stock. *Current Science*, *88*(1), 25–35.

Porter, J. H., Nagy, E., Kratz, T. K., Hanson, P., Collins, S. L., & Arzberger, P. (2009). New eyes on the world: advanced sensors for ecology. *BioScience*, *59*(5), 385–397. doi:10.1525/bio.2009.59.5.6.

Ritsema, C. J., Kuipers, H., Kleiboer, L., van den Elsen, E., Oostindie, K., Wesseling, J. G., et al. (2009). A new wireless underground network system for continuous monitoring of soil water contents. *Water Resources Research*. doi:10.1029/2008wr007071.

Rosenberry, D. O., & Winter, T. C. (1997). Dynamics of water-table fluctuations in an upland between two prairie-pothole wetlands in North Dakota. *Journal of Hydrology*, *191*, 266–289.

Szewczyk, R., Osterweil, E., Polastre, J., Hamilton, M., Mainwaring, A., & Estrin, D. (2004). Habitat monitoring with sensor networks. *Communications of the ACM*, *47*(6), 34–40.

Watras, C. J., Hanson, P. C., Stacy, T. L., Morrison, K. M., Mather, J., Hu, Y.-H., et al. (2011). A temperature compensation method for CDOM fluorescence sensors

- in freshwater. *Limnology and Oceanography: Methods*, 9, 296–301.
- Webster, K. E., Bowser, C. J., Anderson, M. P., & Lenters, J. D. (2006). Understanding the lake-groundwater system: just follow the water. In J. J. Magnuson, T. K. Kratz, & B. J. Benson (Eds.), *Long-term dynamics of lakes in the landscape (Long-Term Ecological Research Network Series)* (pp. 19–48). Oxford: Oxford University Press.
- White, W. N. (1932). *A method of estimating ground-water supplies based on the discharge by plants and evaporation from soils: results of investigations in Escalante Valley, Utah*. U.S. Geol. Surv. Water Supply Paper.